THE JOURNAL OF BIOLOGICAL CHEMISTRY
Vol. 279, No. 38, Issue of September 17, pp. 39331–39339, 2004

Printed in U.S.A.

An Exonic Splicing Enhancer Offsets the Atypical GU-rich 3′ Splice Site of Human Apolipoprotein A-II Exon 3*

Received for publication, May 19, 2004, and in revised form, July 6, 2004
Published, JBC Papers in Press, July 7, 2004, DOI 10.1074/jbc.M405566200

Pablo Arrisi-Mercado‡§, Maurizio Romano‡§¶, Andres F. Muro‡, and Francisco E. Baralle‡‖

From the ‡International Centre for Genetic Engineering and Biotechnology, Padriciano 99, I-34012 Trieste, Italy and the ¶Department of Physiology and Pathology, University of Trieste, Via A. Fleming 22, 34127 Trieste, Italy

Human apolipoprotein A-II (apoA-II) intron 2/exon 3 junction shows a peculiar tract of alternating pyrimidines and purines (GU tract) that makes the acceptor site deviate significantly from the consensus. However, apoA-II exon 3 is constitutively included in mRNA. We have studied this unusual exon definition by creating a construct with the genomic fragment encompassing the whole gene from apoA-II and its regulatory regions. Transient transfections in Hep3B cells have shown that deletion or replacement of the GU repeats at the 3′ splice site resulted in a decrease of apoA-II exon 3 inclusion, indicating a possible role of the GU tract in splicing. However, a 3′ splice site composed of the GU tract in heterologous context, such as the extra domain A of human fibronectin or cystic fibrosis transmembrane conductance regulator exon 9, resulted in total skipping of the exons. Next, we identified the exonic *cis*-acting elements that may affect the splicing efficiency of apoA-II exon 3 and found that the region spanning from nucleotide 87 to 113 of human apoA-II exon 3 is essential for its inclusion in the mRNA. Overlapping deletions and point mutations (between nucleotides 91 and 102) precisely defined an exonic splicing enhancer (ESEwt). UV cross-linking assays followed by immunoprecipitation with anti-SR protein monoclonal antibodies showed that ESEwt, but not mutated ESE RNA, was able to bind both alternative splicing factor/splicing factor 2 and SC35. Furthermore, overexpression of both splicing factors enhanced exon 3 inclusion. These results show that this protein-ESE interaction is able to promote the incorporation of exon 3 in mRNA and suggest that they can rescue the splicing despite the noncanonical 3′ splice site.

Pre-mRNA splicing is the process by which introns are removed and exons are joined together by a two-step *trans*-esterification reaction carried out by the spliceosome, a dynamic 60 S ribonucleoprotein particle (1). Formation of the spliceosome at particular splice junctions is triggered by recognition of the 5′ splice site by the U1 small nuclear ribonucleoprotein and of the 3′ splice site by U2AF followed by the U2 small nuclear ribonucleoprotein recognition of the branch point (2).

The polypyrimidine tract is one of the important *cis*-acting sequences present in the 3′ splice site of introns. The progressive deletion of the polypyrimidine tract abolish lariat formation, spliceosome assembly, and consequently the splicing process (3, 4), whereas increasing the length of the pyrimidine run can lead to improved efficiency of splicing in some systems (4).

In vitro studies have demonstrated that the ability of polypyrimidine tracts to favor specific 3′ splice site selection is not only determined by its length but also by its composition (4, 5). This feature coexists with a degree of flexibility in the specific sequence of a given tract.

The human apolipoprotein A-II (apoA-II)[1] gene presents a peculiar arrangement of GT repeats within the polypyrimidine tract region at the intron 2/exon 3 junction that deviates significantly from the consensus (6). This characteristic GT tract is also found within the intron 8/exon 9 junction of the human CFTR gene, but in this context, it is followed by a polymorphic poly(T) tract (7–9).

This apparent sequence similarity concerning the GU tract is contrasted by the different splicing pattern exhibited by the two genes. In fact, CFTR exon 9 undergoes alternative splicing, and its inclusion is inversely correlated with the length of the GU tract and directly proportional to the length of the poly(T) tract, (7, 10) whereas apparently apoA-II exon 3 is constitutively spliced, and its inclusion is dependent on the presence of the GU tract (11). In other words, in the CFTR intron 8/exon 9 context, the stretch of pyrimidines alternated with purines alone is not equivalent to a functional continuous polypyrimidine tract (10), in contrast to what has been observed for the apoA-II gene (11). Altogether these observations prompted us to investigate the mechanisms underlying the constitutive splicing of apoA-II exon 3 and, in particular, to characterize the *cis*-acting elements and the *trans*-acting factors involved in apoA-II exon 3 definition.

We show here that the third exon of apoA-II contains an exonic splicing enhancer (ESE), which is essential for the inclusion of exon 3 in mRNA and which possibly balances the presence of the noncanonical 3′ splice site. The *trans*-acting factors that target the apoA-II exon 3 ESE have been identified as ASF/SF2 and SC35.

EXPERIMENTAL PROCEDURES

Constructs—To generate the pApo gene system, the full sequence of the gene was obtained by overlapping the PCRs of different fragments from the apoA-II gene (GenBank™ accession number X04898.1) and then cloned XhoI-SacII in pBluescript SK. Each fragment of the complete apoA-II gene was amplified by PCR (94 °C for 30 s, 60 °C for 30 s, 72 °C for 30 s, 30 cycles) using ~200–400 ng of genomic DNA as the

* This work was supported by Grant GGPO2453 from the Telethon Onlus Foundation-Italy (to F. E. B.). The costs of publication of this article were defrayed in part by the payment of page charges. This article must therefore be hereby marked "*advertisement*" in accordance with 18 U.S.C. Section 1734 solely to indicate this fact.

The nucleotide sequence(s) reported in this paper has been submitted to the GenBank™/EBI Data Bank with accession number(s) X04898.1.

§ These authors contributed equally to this paper.

‖ To whom correspondence should be addressed. Tel.: 39-040-3757337; Fax: 39-040-3757361; E-mail: baralle@icgeb.org.

[1] The abbreviations used are: apoA-II, apolipoprotein A-II; ESE, exonic splicing enhancer; EMSA, electrophoretic mobility shift assay; RT, reverse transcription; CFTR, cystic fibrosis transmembrane regulator; SR, serine/arginine-rich; ASF/SF2, alternative splicing factor/splicing factor 2; EDA, extra domain A of human fibronectin.

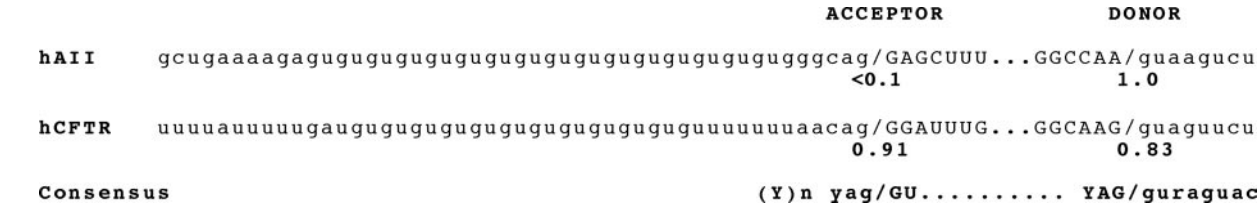

FIG. 1. **Comparison of splice sites of the human apoA-II exon 3 with human CFTR exon 9.** Aligned acceptor and donor splice sites of human apoA-II exon 3 (*hAII*) and human CFTR exon 9 (*hCFTR*) are compared with consensus sequences (*bold lower line*). (*Y*), pyrimidine; (*r*), purine. *Uppercase letters*, exons; *lowercase letters*, introns. The scores for the authentic splice sites (*under the junctions* (/)) were calculated by the SSPNN program (www.fruitfly.org/seq_tools/splice.html).

template. The primer sequences at the 5′ and 3′ extremes of the apoA-II gene were: hapoA-II-1173 XhoI 5′, 5′-tccgctcgagcccgggaggtggaggttgca-3′ and hapoA-II poly(A) SacII 3′, 5′-ttccccgcgggtaggagactctgggtttgga-3′. After amplification, the PCR products were purified through a MicroSpin S-400HR column (Amersham Biosciences AB, Uppsala, Sweden). At position 1549 (intron 2) and 2017 (intron 3), the SalI and EcoRI sites were introduced by PCR-mediated site-directed mutagenesis, respectively, to facilitate subsequent cloning procedures. Also a target sequence was included in the apoA-II expression system at the end of exon 4 to allow the specific amplification and analysis of transfected apoA-II RNA with specific primers.

The CF/apoA-II hybrids were generated by exchanging the SalI-EcoRI cassettes or through a two-step PCR overlap extension. The three constructs with overlapping 21-bp deletions within the exon 3 were generated by exchanging the SalI-EcoRI cassettes in the pApo gene system.

The introduction of artificial point mutations within the ESE in apoA-II exon 3 were carried out by PCR-mediated site-directed mutagenesis. The amplified fragments were digested by SalI-EcoRI and substituted with the appropriate SalI-EcoRI cassettes created in the previously described pApo gene system.

Before expression, the identity of all constructs was checked by a CEQ2000 sequencer (Beckman Coulter, Fullerton, CA) according to the manufacturer's instructions. The wild type polypyrimidine tract of the EDA exon in the α-globin/fibronectin reporter system (12) was replaced by $(GT)_{16}$ repeats. Sense and antisense oligos carrying a $(GT)_{16}$ were designed such that they annealed at the flanking sequences of the EDA polypyrimidine tract. A first PCR reaction (94 °C for 30 s, 60 °C for 30 s, 72 °C for 30 s, for 30 cycles) was performed by using a sense oligo Ex-1S, 5′-atcaaacagaaatgaccattga-3′ annealing at −1 EDA exon and the antisense oligo FN-AII rev, 5′-atcaatgtctgcacacacacacacacacacacacacacacacacactctgttgtg-3′ carrying the $(GT)_{16}$ sequence. A second reaction (same PCR conditions) was carried out by using the sense oligo FN-AII dir, 5′-cacaacagagtgtgtgtgtgtgtgtgtgtgtgtgtgtgcagacattgat-3′ carrying the $(GT)_{16}$ sequence and the antisense oligo Ex+1AS, 5′-ctctttcgggttcacccgca-3′ annealing at +1 EDA exon. Afterward, a third PCR reaction was carried out (same conditions) by using the primers annealing at the extremes Ex − 1S and Ex + 1AS and as a template, 1 μl each of reactions 1 and 2. The final PCR product was visualized in a 1% agarose gel, purified, cloned, and the plasmid transfected in Hep3B cells.

Transfections—The DNA used for transfections was prepared with JetStar purification kit (Genomed, GmbH, Löhne, Germany) following the manufacturer's instructions. Liposome-mediated transfections of 3×10^5 human hepatocarcinoma Hep3B cells were performed using DOTAP liposomal transfection reagent (Alexis Corporation, Lausanne, Switzerland). 3 μg of construct DNA were mixed with 5 μg of DOTAP reagent for each transfection, and the mixture was incubated at room temperature for 15 min to allow the formation of DNA-liposome complexes. The mixture was added to the cells in 3 ml of serum-free culture medium and incubated at 37 °C. After 12 h, the medium was replaced with fresh medium, and 24 h later the cells were harvested. Total RNA was extracted using RNAwiz reagent (Ambion, Austin, TX) and retrotranscribed with poly(dT) primer. To amplify only the messenger derived from the transfections, PCRs were carried out with Ex1–1221 S (5′-accaaggacagagacgctggct-3′) and Not/Cla rev, (5′-tctggacactgcggccgcatcg-3′), which is specific for the construct. The conditions used for the PCRs were the following: 94 °C for 5 min for the initial denaturation, 94 °C for 30 min, 60 °C for 1 min, 72 °C for 1.5 min for 35 cycles, and 72 °C for 7 min for the final extension. The PCRs were optimized to be in the exponential phase of amplification. In some experiments, to quantify the proportion of alternative splicing, cold PCRs were performed for 30 cycles, and then 0.1 μl of α-^{32}P-dCTP (1 μCi) was added to each sample along with 1 unit of Taq. The samples were then amplified for 5 more PCR cycles. Radioactive PCR products were run on 8% denaturant acrylamide gel. Phosphorimaging (Instant Imager, Packard Instrument Co.) was used to quantitate PCR amplifications normalized for the cytidine content in the PCR product sequence.

For the SR protein overexpression experiments, 2 μg of construct pApo-wt or pApo-A97T were cotransfected with 1 and 2 μg of ASF/SF2 and SC35 coding sequences cloned into pCG vector. Each transfection experiment was repeated at least three times.

RNA EMSA and UV Cross-linking of Protein and RNA—For EMSA assays, *in vitro* T7-transcribed ^{32}P-labeled RNAs (4–6 fmol) were incubated with 5.2 mM Hepes, pH 7.9, 1 mM $MgCl_2$, 0.8 mM magnesium acetate, 0.52 mM dithiothreitol, 3.8% glycerol, 0,75 mM ATP, 1 mM GTP, 0.5 μg/μl heparin, and 30 μg of HeLa nuclear extract (4C Biotech, Seneffe, Belgium) in a final volume of 20 μl for 20 min at room temperature. Following the addition of 5 μl of 50% (v/v) glycerol and tracking dye, the complexes were resolved on a 4% polyacrylamide gel (ratio of 19:1 acrylamide:bisacrylamide) in 75 mM Tris-glycine buffer (75 mM Tris, 75 mM glycine) at 15–25 mA for 3–4 h at 4 °C. The gels were dried and exposed to X-OMAT AR films for 1–3 h.

To generate the different versions of human apoA-II exon 3 ESE RNAs, the following oligonucleotides containing the restriction enzymes sites KpnI and HindIII at the 5′ and 3′ splice site, respectively, were used. The sequences were the following: ESEwt, 5′-gg tacctatggcaaggacctgatggagaaggtcaagagaagctt-3′; ESEA97T, 5′-ggtacctatggcaaggacc tgatggtgaaggtcaagagaagctt-3′; and ΔESE-9, 5′-gguaccuauggcaaggaccaggucaagagaagcuu-3′. The oligonucleotides were subcloned in the same restriction sites of pBS SK plasmid, linearized with BamHI, and transcribed *in vitro* in the presence of [α-^{32}P]UTP. The UV cross-linking assay was performed by adding the [α-^{32}P]UTP-labeled RNA probes (1×10^6 cpm/incubation) for 15 min at 30 °C with 20 mg of HeLa nuclear extracts (4C Biotech) in 30 ml of final volume. Final binding conditions were 20 mM Hepes, pH 7.9, 72 mM KCl, 1.5 mM $MgCl_2$, 0.78 mM magnesium acetate, 0.52 mM dithiothreitol, 3.8% glycerol, 0.75 mM ATP, 1 mM GTP, and heparin at a 5μg/μl final concentration as a nonspecific competitor. The samples were then transferred into the wells of a polystyrene plate and irradiated with UV light on ice (800,000 kJ for 5 min). Unbound RNA was then digested with 30 mg of RNase A and 6 units of RNase T1 (Sigma) by incubation at 37 °C for 30 min in a water bath. The samples were then analyzed by 10% SDS-polyacrylamide gel electrophoresis followed by autoradiography.

Immunoprecipitation of SR Proteins following UV Cross-linking—The RNA probes used in this study (ESEwt, ESEA97T, and ΔESE-9) were obtained by cloning SalI-EcoRI in Bluescript SK+, in which the human apoA-II sequence ranged from intron 2 (nucleotide 1549) to intron 3 (nucleotide 2022), with the wild type ESE mutation A97T ESE and ΔESE-9. Each plasmid was then EcoRI-linearized and transcribed *in vitro* in the presence of [α-^{32}P]UTP using T7 RNA polymerase according to standard conditions. The UV cross-linking of labeled RNAs with commercial HeLa nuclear extract was performed as described above. After the 30-min incubation with RNase at 37 °C, 150 μl of immunoprecipitation buffer (20 mM Tris, pH 8.0, 300 mM NaCl, 1 mM EDTA, 0.25% Nonidet P-40) were added to each sample together with 1 μg of monoclonal antibodies and incubated for 2 h at 4 °C on a rotator wheel. Anti-SF2/ASF (monoclonal antibody 96) and Anti-SC35 monoclonal antibodies were purchased from Zymed Laboratories (Zymed Laboratories Inc., San Francisco, CA) and Sigma, respectively. Afterward, 30 μl of protein A7G-Plus-agarose (Santa Cruz Biotechnology, Santa Cruz, CA) were added to each sample and incubated overnight at 4 °C. The beads were subjected to four washing cycles with 1.5 ml of immunoprecipitation buffer and loaded on a 10% SDS-polyacrylamide gel. The gels were run at a constant rate of 30 mA for ~3.5 h, dried, and exposed for 4–6 days with a Biomax Screen (Kodak, Rochester, NY).

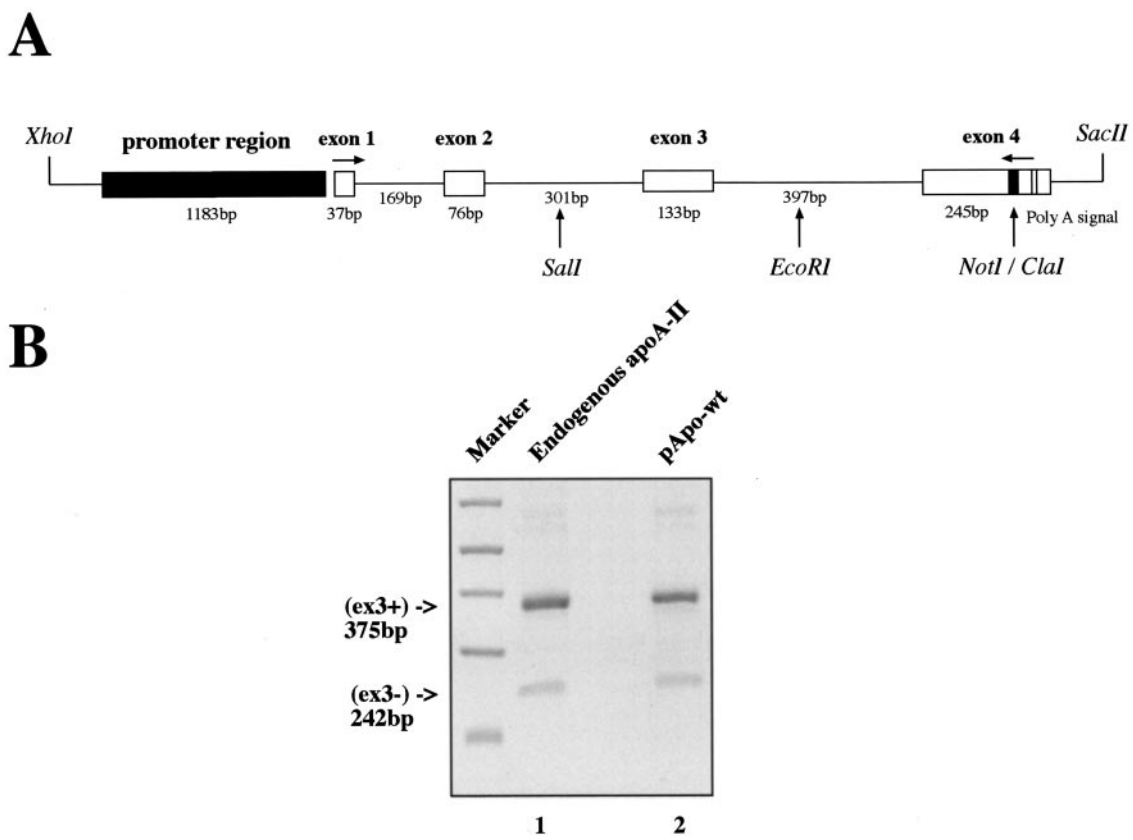

FIG. 2. **Splicing pattern comparison of endogenous apoA-II exon 3 and pApo-wt construct.** *A*, schematic representation of pApo construct. The whole apoA-II gene, from the promoter region to the poly(A) signal, was cloned into the XhoI-SacII sites of the pBluescript plasmid. SalI and EcoRI sites were included in intervening sequences 2 and 3, respectively. The size (in bp) of every exon (*white boxes*) and introns (*solid lines*) as well as position of relevant restriction enzymes target sites are shown. Primers used for RT-PCR are shown as superimposed *arrows* annealing in exon 1 and exon 4. *B*, endogenous apolipoprotein A-II and pApo-wt construct splicing pattern. Analysis of pre-mRNA splicing of the endogenous apolipoprotein A-II gene and pApo construct in Hep3B cell line is shown. The size of the PCR products including (*ex3+*, 375 bp) and excluding (*ex3−*, 242 bp) exon 3 are indicated. Amplicons were separated on 2.0% (w/v) agarose gel. The primers used for PCR amplification of the endogenous apoA-II were Ex 1–1221 S and Rev Cla/Not, whereas for pApo-wt, Ex 1–1221 S and Not/Cla rev were used.

RESULTS

Analysis of the ApoA-II Exon 3—As a first approach, we studied the association between the splice site strength and the different splicing behaviors of human apoA-II exon 3 and human CFTR exon 9. This was done by computer in a comparative sequence analysis of the 5′ and 3′ splice sites of the human apoA-II exon 3 and human CFTR exon 9.

The strength of these splice sites was calculated according to the Splice Site Prediction by Neural Network program (SSPNN, www.fruit fly.org/seq_tools/splice.html). In general, sequences that have a high score are considered to be strong (the maximum is 1.0 and corresponds to the consensus sequence). The program found the authentic 5′ and 3′ splice sites of human CFTR exon 9 (T7 version of the polypyrimidine tract) in which the scores were 0.83 and 0.91, respectively (Fig. 1).

The calculated scores for the human apoA-II exon 3 demonstrated that the authentic donor splice site is ranked as the best possible 5′ splice site (score = 1.0) within the 600 bp encompassing the genomic region between apoA-II exon 2 and exon 3. On the other hand, the authentic 3′ splice site of apoA-II exon 3 is not ranked among the possible 3′ splice sites within the same genomic region (at least with both donor and acceptor cut-off at 0.1). Five cryptic 3′ splice sites (in which scores ranged from 0.11 up to 0.99) were also identified, (not shown). Overall, these observations suggest that the authentic acceptor splice site of human apoA-II exon 3 might be weak because of the presence of the noncanonical (GU) dinucleotide repeats within the 3′ splice site.

The apparent weakness of the human apoA-II exon 3 acceptor splice site (strength <0.1) in comparison with the human CFTR exon 9 acceptor splice site (strength = 0.91) is in striking contrast with the splicing behavior of the two exons. In fact, human apoA-II exon 3 is constitutively included in mRNA; whereas human CFTR exon 9 is alternatively spliced. Hence, it is plausible that novel accessory *cis*-acting elements might be involved in the apoA-II exon 3 definition to support its constitutive splicing.

In Vivo System for the Study of ApoA-II Exon 3 Splicing—To study the relevance of the splice site strength and map the possible *cis*-acting elements involved in the apoA-II exon 3 definition, we generated a eukaryotic gene expression system by cloning the whole 3.2-kbp apoA-II gene including the promoter region and its polyadenylation site (pApo-wt) (Fig. 2*A*).

In comparison with the minigene system widely used to study other splicing models (13–17), where only one exon and its flanking regions are cloned in a heterologous gene context, the apoA-II expression system that we generated contains most of the elements necessary for its transcription and RNA processing, which are also present in the endogenous apoA-II gene. Such a construct should allow the study of the *cis*-acting elements affecting apoA-II exon 3 splicing in a context as close as possible to the chromosomal background.

The transient transfection of the pApo-wt gene system in Hep3B cells was followed by reverse transcription (RT) using a primer specific for the pApo-wt construct or the endogenous gene. The splicing pattern was then determined by PCR amplification using primers that recognized slightly modified se-

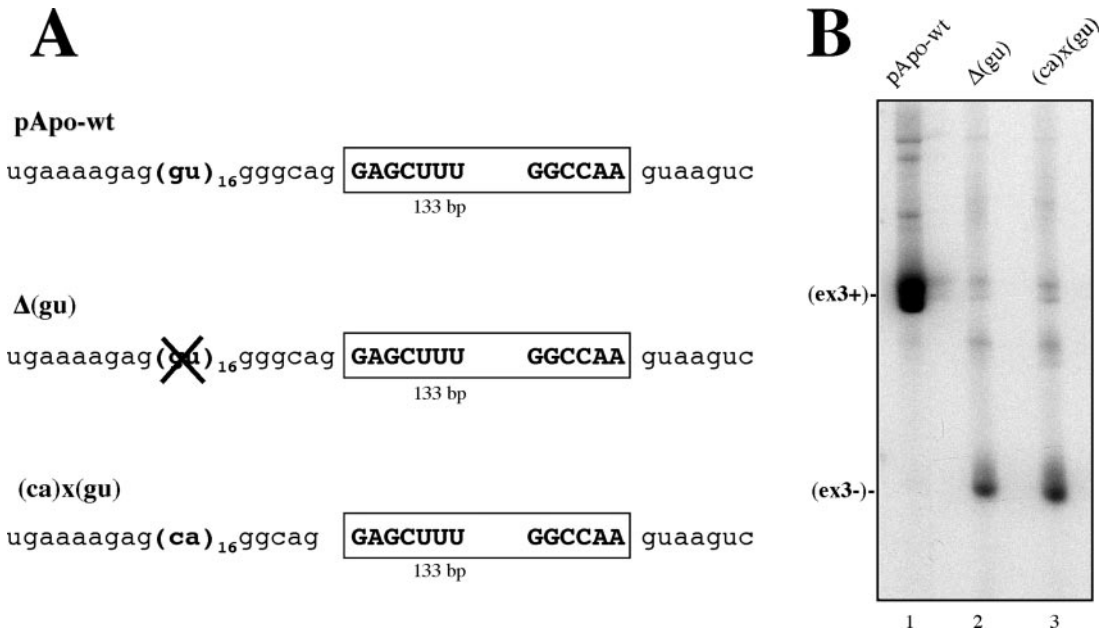

FIG. 3. ***In vivo* effect of GU deletion/replacement.** *A*, partial sequence of exon 3 and flanking introns showing the modifications within the 3′ splice site. *B*, denaturing acrylamide gel of radioactive RT-PCRs of pre-mRNA splicing pattern of human apoA-II constructs in Hep3B cells. The relevance of the GU tract at the 3′ splice site of exon 3 was assessed by deletion and replacement by the CA tract. The relative amount of exon 3 skipping (*ex3−*) was quantified by phosphorimaging analysis of the radioactive PCRs as described under "Experimental Procedures." Δ(gu) = 90%; (ca)x(gu) = 95%. Standard deviations were <5%.

quences in the plasmid pApo-wt, which allowed us to discriminate its transcript from the endogenous one.

Fig. 2*B* shows that the splicing efficiency of the apoA-II construct in Hep3B cells was similar to that observed for the endogenous apoA-II gene, displaying about 90% of exon 3 inclusion. An identical experimental strategy was used in all of the following experiments using mutated versions of the pApo-wt gene construct.

In Vivo Effects of $(GT)_{16}$ Tract Deletion and Replacement—We have shown previously that when the U tract is removed from human CFTR intron 8, total exon 9 exclusion occurs (10). Moreover, an increase of the number of (GU) dinucleotide repeats reduces the efficiency of exon 9 inclusion. This splicing pattern is in contrast with what is observed in the apoA-II context, where exon 3 inclusion reaches 90%. Therefore, in the context of apoA-II, the (GU) dinucleotide repeats seem to work as a functional polypyrimidine tract. To test this hypothesis, we deleted all the (GT) dinucleotide repeats from the apoA-II intron 2 (Fig. 3*A*, construct *Δ(gu)*). As a control, a sequence containing $(CA)_{16}$ dinucleotide repeats was used to replace the $(GT)_{16}$ tract maintaining the same length (Fig. 3*A*, construct *(ca)x(gu)*). The deletion and replacement of the (GU) tract resulted in almost 100% of exon 3 being excluded (Fig. 3*B*, *lanes 2* and *3*). This result supports previous studies showing that the removal of all the GU repeats in the apoA-II intron 2 caused ~90% of exon 3 to be skipped (11).

To establish if the GU tract is functional or detrimental in systems different from the exons under study (apoA-II exon 3 and CFTR exon 9), we have tested the effect of replacing a canonical polypyrimidine tract with GU repeats. Using a minigene system for the mouse fibronectin EDA exon (12), we found that the substitution of the EDA exon polypyrimidine tract with the apoA-II $(GT)_{16}$ tract resulted in 95% of the EDA exon being excluded (Fig. 4).

Altogether these results indicate that the $(GU)_{16}$ tract functions as a polypyrimidine tract, which depends on its context and location in the nucleotide sequence. Moreover, these data suggest that the 3′ splice site definition of the apoA-II exon 3 might be supported by strong and specific *cis*-acting elements

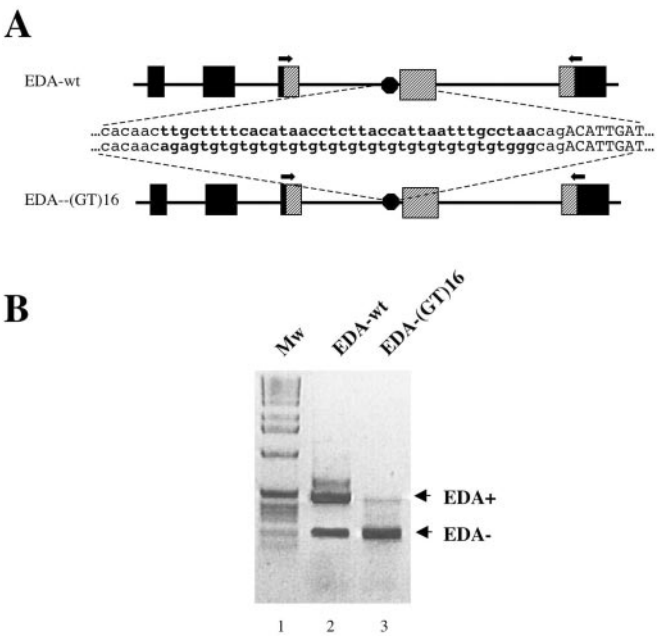

FIG. 4. **Effects of apoA-II-$(GU)_{16}$ replacement within the polypyrimidine tract of mouse EDA exon.** *A*, schematic representation of the α-globin/fibronectin reporter system used to test the apoA-II $(GU)_{16}$ polypyrimidine tract in a heterologous system. α-Globin and fibronectin EDA exons are indicated in *black* and *gray*, respectively. The *black circles* indicate the polypyrimidine tracts. The primers used in the RT-PCR assay are indicated by the superimposed *arrows*. The sequences of the mouse EDA and the apoA-II exon 3 polypyrimidine tracts are shown. *B*, splicing pattern analysis by ethidium bromide staining of a 2% agarose gel electrophoresis of the RT-PCR product derived from cellular RNA. The replacement of the EDA polypyrimidine tract with the apoA-II tract led to 95% EDA exclusion.

that counteract the effect of the noncanonical polypyrimidine tract.

Mapping of Regulatory Elements within ApoA-II Exon 3—To identify regulatory elements placed within the apoA-II exon 3, we generated hybrid constructs between apoA-II exon 3 and

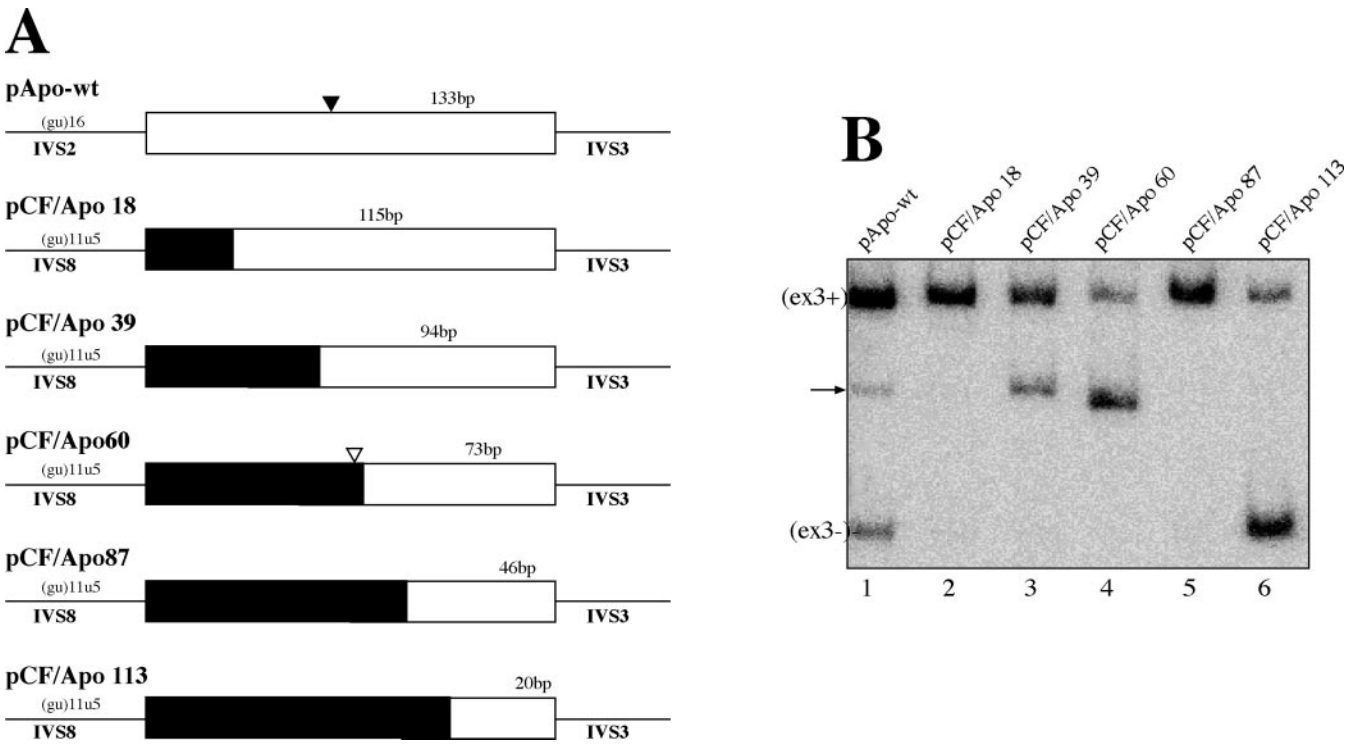

FIG. 5. **Effect of the progressive apoA-II exon 3 replacement by CFTR exon 9.** *A*, the schemes of the CFTR IVS8-exon 9 (*black*)/apoA-II exon 3-IVS3 (*white*) hybrid constructs used for transient transfections in Hep3B cells are shown. The size (in bp) of these replacements is also indicated. Cryptic splice sites of apoA-II exon 3 (56 nucleotides downstream of the acceptor site) and CFTR exon 9 (previously characterized) are shown with a *black* and *white arrowhead*, respectively. *IVS*, intervening sequence. *B*, denaturing acrylamide gel of radioactive RT-PCRs of the pre-mRNA splicing pattern of the CFTR/apoA-II hybrid constructs. The *horizontal arrow* on the RT-PCR results indicates aberrant splicing products originated from cryptic 3′ splice sites located in the hybrid exon 3. The relative amount of exon 3 skipping (*ex3*−) was quantified by phosphorimaging analysis of radioactive PCRs as described under "Experimental Procedures." pApo-wt = 10%; pCF/apo113 = 80%. Standard deviations were <10%.

CFTR exon 9 in the same manner as the splicing regulatory elements of CFTR exon 9 had been previously characterized (18).

A set of five CFTR/apoA-II hybrids was generated in which the exon 3 was progressively replaced by CFTR exon 9 and its 3′ splice site replaced with the allelic configuration $(GT)_{11}(T)_5$. The constructs were named by indicating the number of apoA-II exon 3 nucleotides replaced by CFTR exon 9 (*i.e.* 18, 39, 60, 87, and 113) (Fig. 5*A*).

In comparison with the splicing pattern of pApo-wt, the pCF/Apo18 construct showed 100% of exon 3 inclusion, thus supporting the hypothesis that the CFTR $(GT)_{11}(T)_5$ polypyrimidine tract is stronger than that of the apoA-II $(GT)_{16}$ (Fig. 5*B*, *lanes 1* and *2*). Subsequently, the pCF/Apo39 showed an increase in the cryptic splice site usage (this cryptic splice site is located 56 nucleotides downstream of the 3′ splice site of apoA-II exon 3, which is observed as a faint band in apoA-II wild type) (Fig. 5*B*, *lane 3*). On the other hand, the pCF/Apo60 constructs showed a new cryptic 3′ splice site introduced with the extension of the CFTR sequence from nucleotides 39 to 60 (Fig. 5*B*, *lane 4*). This cryptic splice site has been characterized previously (10). The transfection of the pCF/Apo87 construct showed 100% inclusion of exon 3, whereas the pCF/Apo113 construct showed 80% exclusion of exon 3 (Fig. 5*B*, *lanes 5* and *6*). In principle, the strikingly different splicing patterns of pCF/Apo87 and pCF/Apo113 constructs might be due to the removal of an enhancer element placed within the 26 bp of the apoA-II exon or to the addition of a silencer element introduced within the 26 bp of the CFTR exon 9. However, considering that previous mapping studies did not highlight the presence of any exonic CFTR regulatory element in this 26-bp range (18), we focused attention on the enhancer-like sequence possibly present in the removed sequences of apoA-II exon 3. To identify the nucleotides within this 26-bp region that contributed to efficient exon 3 splicing, we constructed three 21-bp overlapping deletions encompassing the 26-bp sequence (Fig. 6*A*). The three constructs (Δ1843–63, Δ1854–74, Δ1866–86) were transiently expressed in Hep3B, and the RNA was analyzed by RT-PCR.

The Δ1843–63 deletion caused 80% of exon 3 exclusion, whereas both the Δ1854–74 and the Δ1866–86 deletions resulted in 55% of exon 3 exclusion (Fig. 6*B*). Therefore, the region spanning from nucleotide 1843 to 1886 seems to affect positively apoA-II exon 3 definition. In previous studies, a broad spectrum of enhancer-like sequences capable of promoting exon inclusion have been identified (19). Interestingly, the motif GGAGA (Class I of purine-rich enhancers) is also present in the 1856–1860 nucleotide region of apoA-II exon 3. Moreover, the 1852–1856 region is compatible with the ASF/SF2 motifs found through functional systematic evolution of ligands by exponential enrichment (SELEX) (20). Therefore, we focused attention on the sequence ranging from nucleotide 1852 to 1860 (corresponding to nucleotides 91–99 of exon 3) to be analyzed as a possible regulatory element (Fig. 7*A*, *boxed*). To map finely which base(s) in such a region was directly affecting exon 3 definition, point mutations were introduced within this 9-bp region. Each base, one at a time, was replaced by its complementary one, generating nine different constructs that were used to transfect the Hep3B cell line (Fig. 7*B*). Although most of the substitutions did not have a significant effect on exon 3 processing in Hep3B cells, G92C, A99T, and more noticeably, A97T caused 20, 60, and 85% of exon 3 skipping, respectively (Fig. 7*C*, *lanes 3*, *8*, and *10*).

Interaction of SR Proteins with apoA-II 9-Nucleotide ESE—To identify the *trans*-acting factors able to bind the

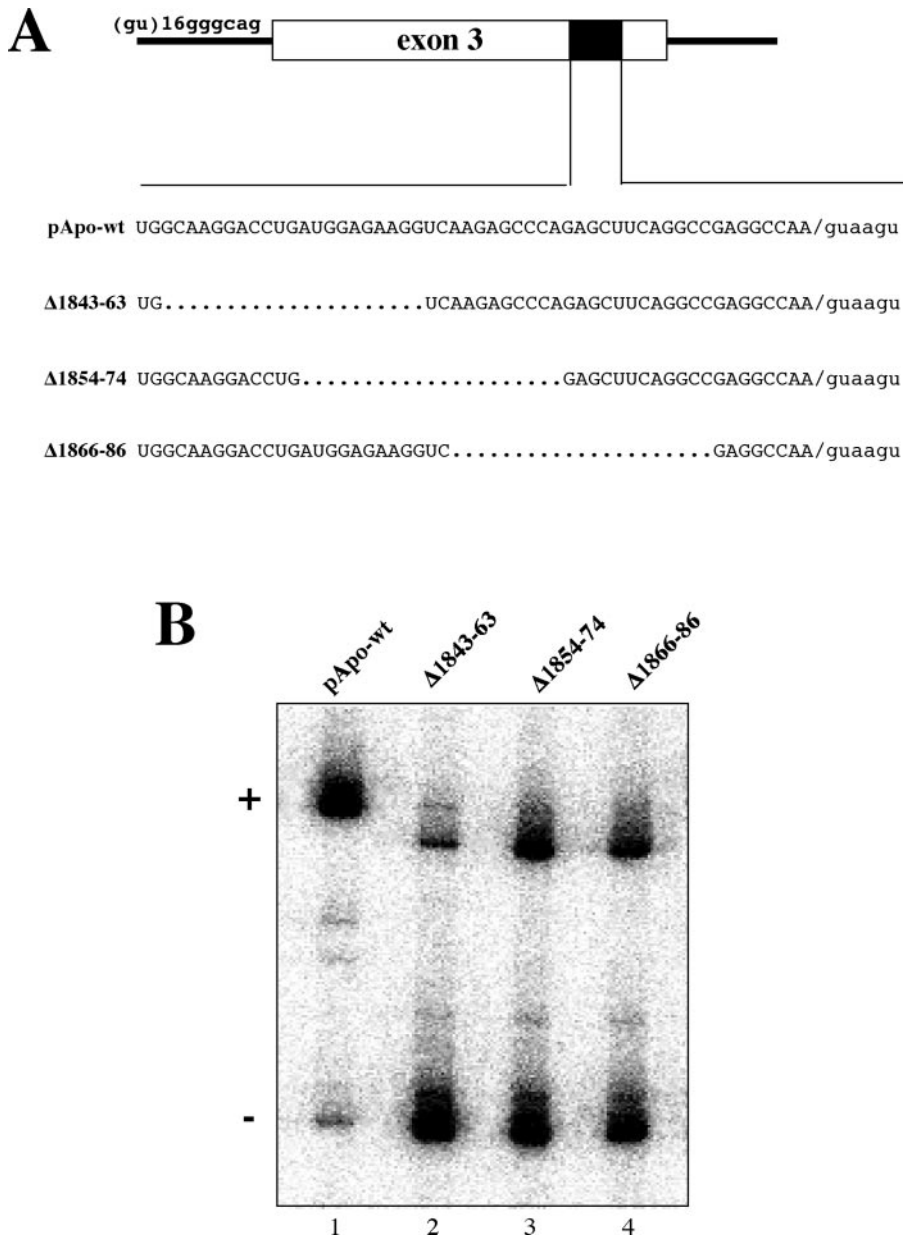

FIG. 6. **Effect of the overlapping deletions within the apoA-II exon 3.** *A*, scheme and sequence of the overlapping 21-nucleotide deletions within apoA-II exon 3. *B*, denaturing acrylamide gel of radioactive RT-PCRs of the pre-mRNA splicing pattern of the overlapping deletion constructs. The three 21-nucleotide deletions within apoA-II exon 3 led to exon 3 skipping. The relative amount of exon 3 skipping (*ex3*−) was quantified by phosphorimaging analysis of radioactive PCRs as described under "Experimental Procedures." pApo-wt = 10%; Δ1843–63 = 80%; Δ1854–74 = 55%; Δ1866–86 = 55%. Standard deviations were <10%.

9-nucleotide enhancer-like sequence within apoA-II exon 3, both EMSA and UV cross-linking assays were performed. For the EMSA experiment, we used *in vitro* transcribed RNAs including the 9-nucleotide wild type core region of the apoA-II exon 3 (ESEwt) or this same sequence point-mutated (ESE A97T) or deleted (ΔESE-9) (Fig. 8*A*). The RNAs were incubated with HeLa nuclear extract in the presence of the nonspecific competitor heparin (see "Experimental Procedures"). As shown in Fig. 8*B*, ESEwt RNA showed a broad band of shifted material, which is slightly weaker with the ESE-A97T RNA and almost nonexistent with the ΔESE-9 RNA (*lanes 4–6*). Nevertheless, it should be noted that the region used as the EMSA probe spans the deletion of Δ1843–63 and Δ1854–74. Therefore, these results suggest that several proteins might interact specifically with the wild type apoA-II exon 3 across the 9-nucleotide sequence and its flanking regions, which explains the minimal differences between the ESEwt and ESEA97T complexes observed in the gel shift assay.

The nature of the protein(s) that bind(s) to the wild type apoA-II exon 3 across the 9-nucleotide sequence was then investigated by UV cross-linking of RNA-protein complexes. ^{32}P-labeled ESEwt, A97T, and ΔESE-9 RNA probes were incubated with HeLa nuclear extract and were cross-linked to proteins by exposure to UV light. The resulting ^{32}P-labeled protein(s) was (were) separated by SDS-PAGE. The pattern of UV cross-linked proteins obtained with these three different constructs did not display any significant difference (data not shown).

To test the possible differential recruitment of SR proteins by the wild type, mutated, or deleted apoA-II 9-nucleotide ESE that may be obscured in the UV cross-linking assay, these were followed by immunoprecipitation with anti-SR protein monoclonal antibodies. The constructs used for these experiments carry ESEwt, ESE A97T, and ΔESE-9 (Fig. 9*A*).

The immunoprecipitation of the UV cross-linked material with monoclonal antibody 1H4 directed against SRp40, SRp55, and SRp75 did not produce any specific immunoprecipitated material (not shown). Instead, the monoclonal antibody 96 anti-SF2/ASF monoclonal antibody (Fig. 9*B*, *left panel*) and anti-SC35 monoclonal antibody (*right panel*) immunoprecipitated specific proteins (*lanes 1*) following UV cross-linking with nuclear extract of a labeled ESEwt RNA but only traces with the ESE A97T and ΔESE-9 control RNAs (*lanes 2* and *3*). Thus,

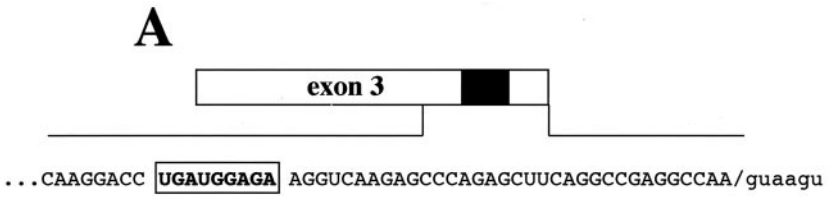

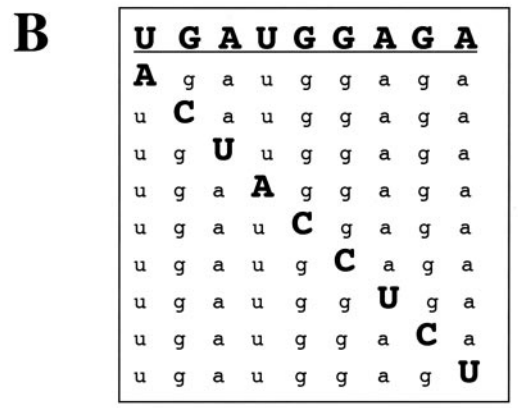

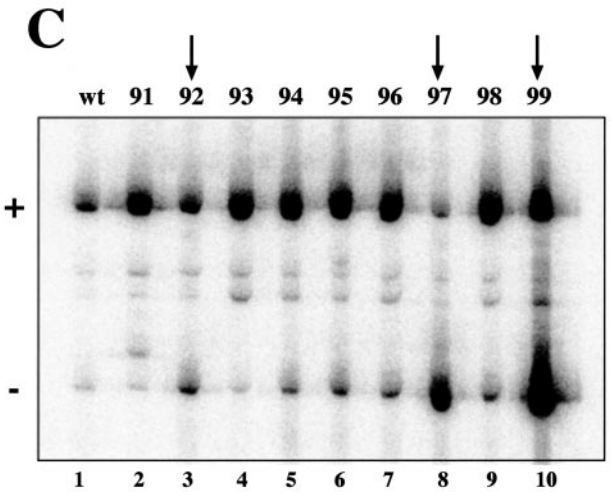

FIG. 7. **Effect of point mutations within the apoA-II exon 3 putative ESE.** *A*, scheme of apoA-II exon 3 and partial sequence containing the ESE sequence (*box*). *B*, scheme of the point mutations that were carried out. Briefly, each base at a time in the ESE was replaced by its complement. Changes are indicated in *bold capital letters* (*diagonal*). *C*, denaturing acrylamide gel of radioactive RT-PCRs of pre-mRNA splicing pattern of the point-mutated pApo constructs. *Black arrows* indicate the strongest effects of the point mutations on exon 3 skipping (*left to right*, G92C, A97T, and A99T). The relative amount of exon 3 skipping (*ex3−*) was quantified by phosphorimaging analysis of radioactive PCRs as described under "Experimental Procedures." G92C = 20%; A97T = 85%; A99T = 60%. Standard deviations were <15%.

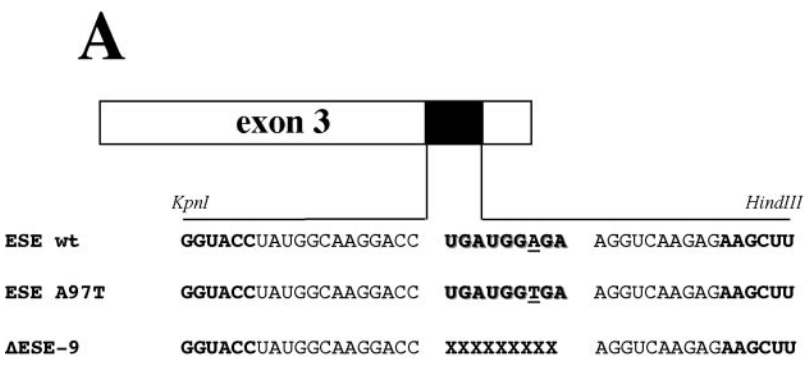

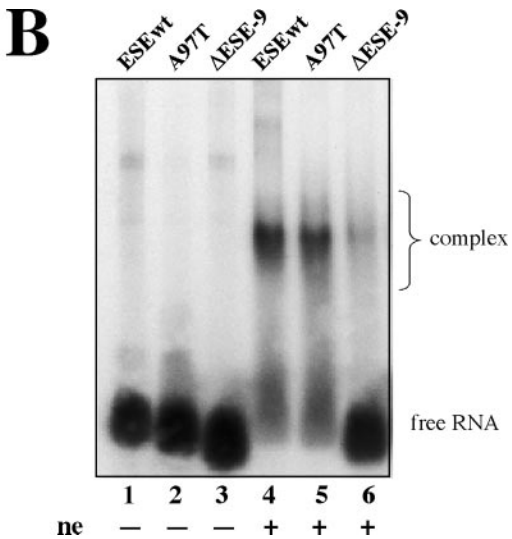

FIG. 8. **Electrophoretic mobility shift assay with apoA-II exon 3 ESE RNA.** *A*, scheme of the constructs carrying wild type (*ESEwt*), point-mutated (*ESE A97T*), and deleted (Δ*ESE-9*) exonic splicing enhancer of *apoA-II* exon 3 used for the EMSA. *B*, radiolabeled RNAs were incubated with HeLa nuclear extract (*ne*) for 20 min at room temperature. Complexes were then fractionated on a 4% nondenaturing polyacrylamide gel. The position of bound (*complex*) or free RNA is indicated.

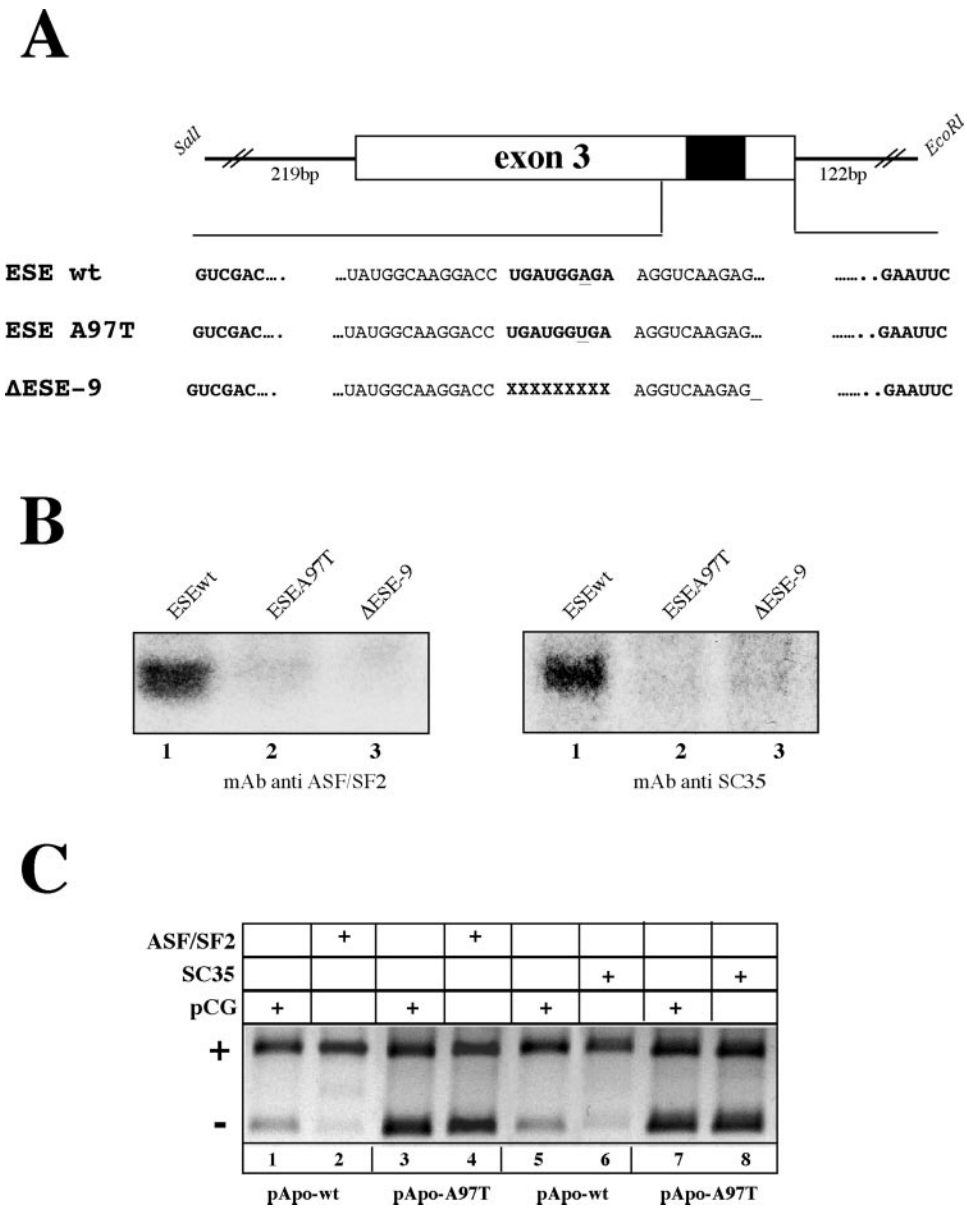

FIG. 9. **SR proteins and apoA-II exon 3 enhancer.** *A*, partial sequence of the constructs used for UV cross-linking followed by immunoprecipitation. Three constructs containing exon 3 with the intact, point-mutated, and deleted ESE (*ESEwt*, *ESE A97T*, and Δ*ESE-9*, respectively) plus portions of the flanking introns 2 and 3 are shown. *B*, 10% SDS-PAGE analysis of immunoprecipitation with an anti-ASF/SF2 (*left panel*) and anti-SC35 (*right panel*) monoclonal antibodies following UV cross-linking of the labeled RNAs ESEwt, ESEA97T, and ΔESE-9. *C*, effects of ASF/SF2 and SC35 overexpression on apoA-II exon 3 inclusion.

these results provide evidence that at least two SR proteins are able to interact with the nucleotides across the ESE sequence and are also consistent with the result obtained in the EMSA study, where a clear difference in the RNA-protein complex formation with a construct containing the ESEwt and ΔESE-9 is observed.

Effect of ASF/SF2 and SC35 Overexpression on Splicing of ApoA-II Exon 3—To highlight the putative positive effect of ASF/SF2 and SC35, plasmids containing the open reading frame of these SR proteins were cotransfected along with pApo-wt construct. Thus, the possible positive effects of the overexpression of ASF/SF2 and/or SC35 should cause an increase of exon 3 inclusion, even though the percentage of basal exon 3 skipping is low (about 10%). As a control, the construct carrying the point mutation A97T within the ESE was used (pApo-A97T). Fig. 9*C* showed that the cotransfection of pApo-wt with ASF/SF2 (*lane 2*) and SC35 (*lane 6*) promoted exon 3 inclusion when compared with the cotransfection with the empty vector pCG (*lanes 1* and *5*). Conversely, the cotransfection of ASF/SF2 and SC35 with the construct carrying the A97T point mutation showed no significant variation in levels of exon 3 inclusion (Fig. 9*C*, *lanes 4* and *8*). Altogether these results confirm that the disruption of the ESE by the point mutation A97T prevents a functional binding of ASF/SF2 and SC35 to this regulatory sequence and inhibits the positive effect. Hence, both ASF/SF2 and SC35, in which specific interaction to the ESE had already been demonstrated by UV cross-linking/immunoprecipitation (Fig. 9*B*), have a functionally positive effect, increasing the apoA-II exon 3 inclusion.

DISCUSSION

Human apoA-II exon 3 and its flanking introns share only partially the canonical features of splicing sites. In fact, the 5′ splice site of intron 3 is well defined and resembles the consen-

sus sequences (21), whereas the 3′ splice site of intron 2 contains a polymorphic sequence made of alternating pyrimidines and purines, instead of the classical polypyrimidine tract.

The comparison of splice sites strength of human apoA-II exon 3 and human CFTR exon 9 has delineated an apparent contradiction between the splicing behavior of the two exons and the strength of the splice sites. Taking advantage of the compact size of the human apoA-II gene, we were able to create an *in vivo* expression system that includes the whole 1173-bp enhancer promoter region in which the 1226-bp coding region encompasses 4 exons and 3 introns and the 320-bp 3′-UTR (where the polyadenylation signal is located). In this way, it was possible to study the exon 3 splicing within a context very similar to the chromosomal context. In addition, a liver-derived cell line (Hep3B) was used to provide a cellular context more similar to that of original tissue where the apoA-II gene is normally expressed. This represents a clear advantage in comparison with the minigene system and is widely used to study other splicing models where only one or a few exons and their flanking regions are cloned in a heterologous gene context.

The first approach toward the characterization of the *cis*-acting elements involved in the apoA-II exon 3 definition led to confirmation of the relevance of the (GU) tract in our system. Both the deletion or the replacement of the $(GU)_{16}$ tract with its complementary $(CA)_{16}$ tract resulted in 90% exclusion of exon 3 from apoA-II mRNA. It is well known that there is great flexibility in the specific sequence within the polypyrimidine tract. In fact, it has been shown that the introduction of purines into the polypyrimidine tract is detrimental to splicing only if the length of the tract is shortened and if there is a reduction in the number of consecutive uridine residues (4, 22, 23).

Our *in vivo* results are consistent also with previous *in vitro* studies on tracts containing alternating pyrimidine and purine residues, which found that they are functional (5). In contrast, we demonstrated that the replacement of the authentic polypyrimidine tract of the mouse fibronectin EDA exon with the apoA-II $(GU)_{16}$ polypyrimidine tract produced EDA exon skipping; therefore, the GU tract is not functionally equivalent *in vivo* to a polypyrimidine tract in a context different from the apoA-II intron 2.

A possible explanation for the ability of the (GU) repeats to work as a functional polypyrimidine tract derives from the combinatorial action of the *cis*-acting elements that drive the selection of 3′ splice sites. It is clear that the strength of the adjacent branch point also plays an important role in splice site selection (3, 24). Moreover, studies on regulated alternative splicing have identified exonic splicing elements that facilitate the process of exon definition. Therefore, functional exon definition depends also on the presence of exon enhancers that can clearly rescue splicing from otherwise weak 3′ splice sites (25–28). It is now clear that ESEs are not only components of regulated exons but also of constitutively spliced exons (29, 30).

The progressive replacement of apoA-II by CFTR sequences led to the identification of a region between nucleotides 87 to 113 of human apoA-II exon 3 as essential for its inclusion in mRNA. On the basis of previous functional studies, which identified different classes of splicing enhancers (20, 30), we have outlined a putative enhancer-like sequence located in the region spanning from nucleotide 91 to 99 of exon 3 that was further characterized through mapping by point mutations. Considering the base composition of this 9-bp region (TGATGGAGA), this sequence would belong to a purine-rich ESE category.

Our UV cross-linking coupled with immunoprecipitation experiments showed the ability of the wild type, but not of the A97T ESE, sequences to bind ASF/SF2 and SC35. The relevance of the these two splicing factors for apoA-II exon 3 splicing is confirmed also by *in vivo* SR protein overexpression experiments. In conclusion, our results indicate that the noncanonical polypyrimidine tract of the apoA-II intron 2 is balanced by the presence of at least one enhancer-like sequence placed within exon 3.

We have shown that ESE is bound by ASF/SF2 and SC35, which, in turn, may have a pivotal role in recruiting the constitutive splicing factor U2AF65, which does not have available a canonical polypyrimidine tract. These data support the hypothesis that the weak polypyrimidine tract of intron 2 might be unable to recruit directly the constitutive splicing factors even in the presence of a strong 5′ splice site.

A large body of evidence indicates that U2AF35 is required for constitutive splicing and also works as a mediator of enhancer-dependent splicing (31–33). *In vitro* protein-RNA interaction studies with pre-mRNAs containing either a constitutive or regulated splicing enhancer have shown that U2AF35 directly mediates interactions between U2AF65 and proteins bound to the enhancers (34). Thus, U2AF35 should recruit U2AF65 acting as a bridge between these proteins and the enhancer complex. In the case of apoA-II exon 3, this recruitment should be mediated by the ESE sequence characterized in this paper and its interactions with ASF/SF2 and SC35.

Acknowledgments—We thank Dr. Emanuele Buratti for helpful suggestions and comments and Dr. Maurizio Giombi for technical help.

REFERENCES

1. Staley, J. P., and Guthrie, C. (1998) *Cell* **92,** 315–326
2. Black, D. L. (2003) *Annu. Rev. Biochem.* **72,** 291–336
3. Mullen, M. P., Smith, C. W., Patton, J. G., and Nadal-Ginard, B. (1991) *Genes Dev.* **5,** 642–655
4. Roscigno, R. F., Weiner, M., and Garcia-Blanco, M. A. (1993) *J. Biol. Chem.* **268,** 11222–11229
5. Coolidge, C. J., Seely, R. J., and Patton, J. G. (1997) *Nucleic Acids Res.* **25,** 888–896
6. Shelley, C. S., Sharpe, C. R., Baralle, F. E., and Shoulders, C. C. (1985) *J. Mol. Biol.* **186,** 43–51
7. Chu, C. S., Trapnell, B. C., Curristin, S., Cutting, G. R., and Crystal, R. G. (1993) *Nat. Genet.* **3,** 151–156
8. Cuppens, H., Teng, H., Raeymaekers, P., De Boeck, C., and Cassiman, J. J. (1994) *Hum. Mol. Genet.* **3,** 607–614
9. Dork, T., Fislage, R., Neumann, T., Wulf, B., and Tummler, B. (1994) *Hum. Genet.* **93,** 67–73
10. Niksic, M., Romano, M., Buratti, E., Pagani, F., and Baralle, F. E. (1999) *Hum. Mol. Genet.* **8,** 2339–2349
11. Shelley, C. S., and Baralle, F. E. (1987) *Nucleic Acids Res.* **15,** 3787–3799
12. Muro, A. F., Iaconcig, A., and Baralle, F. E. (1998) *FEBS Lett.* **437,** 137–141
13. Vibe-Pedersen, K., Kornblihtt, A. R., and Baralle, F. E. (1984) *EMBO J.* **3,** 2511–2516
14. Webb, K. E., Martin, J. F., Cotton, J., Erusalimsky, J. D., and Humphries, S. E. (2003) *Exp. Hematol.* **31,** 488–494
15. Shin, D., Park, S., and Park, C. (2003) *Biochem. J.* **374,** 175–184
16. Kwok, J. B., Halliday, G. M., Brooks, W. S., Dolios, G., Laudon, H., Murayama, O., Hallupp, M., Badenhop, R. F., Vickers, J., Wang, R., Naslund, J., Takashima, A., Gandy, S. E., and Schofield, P. R. (2003) *J. Biol. Chem.* **278,** 6748–6754
17. Muro, A. F., Caputi, M., Pariyarath, R., Pagani, F., Buratti, E., and Baralle, F. E. (1999) *Mol. Cell. Biol.* **19,** 2657–2671
18. Pagani, F., Buratti, E., Stuani, C., Romano, M., Zuccato, E., Niksic, M., Giglio, L., Faraguna, D., and Baralle, F. E. (2000) *J. Biol. Chem.* **275,** 21041–21047
19. Schaal, T. D., and Maniatis, T. (1999) *Mol. Cell. Biol.* **19,** 1705–1719
20. Liu, H. X., Zhang, M., and Krainer, A. R. (1998) *Genes Dev.* **12,** 1998–2012
21. Lopez, A. J. (1998) *Annu. Rev. Genet.* **32,** 279–305
22. Reed, R. (1989) *Genes Dev.* **3,** 2113–2123
23. Norton, P. A. (1994) *Nucleic Acids Res.* **22,** 3854–3860
24. Reed, R., and Maniatis, T. (1988) *Genes Dev.* **2,** 1268–1276
25. Lavigueur, A., La Branche, H., Kornblihtt, A. R., and Chabot, B. (1993) *Genes Dev.* **7,** 2405–2417
26. Watakabe, A., Tanaka, K., and Shimura, Y. (1993) *Genes Dev.* **7,** 407–418
27. Xu, R., Teng, J., and Cooper, T. A. (1993) *Mol. Cell. Biol.* **13,** 3660–3674
28. Tanaka, K., Watakabe, A., and Shimura, Y. (1994) *Mol. Cell. Biol.* **14,** 1347–1354
29. Mayeda, A., Badolato, J., Kobayashi, R., Zhang, M. Q., Gardiner, E. M., and Krainer, A. R. (1999) *EMBO J.* **18,** 4560–4570
30. Schaal, T. D., and Maniatis, T. (1999) *Mol. Cell. Biol.* **19,** 261–273
31. Graveley, B. R., Hertel, K. J., and Maniatis, T. (2001) *RNA* (*N. Y.*) **7,** 806–818
32. Blencowe, B. J. (2000) *Trends Biochem. Sci.* **25,** 106–110
33. Zhu, J., and Krainer, A. R. (2000) *Genes Dev.* **14,** 3166–3178
34. Zuo, P., and Maniatis, T. (1996) *Genes Dev.* **10,** 1356–1368